Eur. J. Biochem. 224, 951–957 (1994)


# Identification of functional domains in the cytoskeletal protein talin

Verena NIGGLI[1], Stephan KAUFMANN[2], Wolfgang H. GOLDMANN[2], Thomas WEBER[3] and Gerhard ISENBERG[2]

[1] Department of Pathology, University of Bern, Switzerland
[2] Biophysics Department E-22, Technical University of Munich, Germany
[3] Department of Biochemistry, Swiss Federal Institute of Technology, Zürich, Switzerland

(Received May 27, 1994) – EJB 94 0760/3

The cytoskeletal protein talin potentially plays a key role in actin–membrane linkage. It is able to nucleate actin filament growth *in vitro* while binding simultaneously to lipid bilayers. Thrombin digestion of human platelet talin yields two polypeptide domains of 200 kDa and 47 kDa. We have purified these fragments and analyzed their functional properties: the 200-kDa fragment was active in nucleating actin filament formation and reduced the viscosity of filamentous actin, comparable to the effects of the intact protein. The 47-kDa fragment was inactive in this respect.

However, the 47-kDa polypeptide, but not the 200-kDa fragment, interacted specifically with large liposomes containing acidic phospholipids. This is demonstrated by selective, hydrophobic photolabeling of the 47-kDa fragment using phosphatidylserine liposomes containing trace amounts of a photoactivatable phospholipid analogue and by selective co-sedimentation of this domain with the liposomes. The 200-kDa fragment, whether alone or in conjunction with the small fragment, neither incorporated significant amounts of label nor co-sedimented with the liposomes.

We thus are able to attribute specialized functions to distinct domains on the talin molecule. These enable the protein to interact simultaneously with actin filaments and lipid membranes.

The cytoskeletal protein talin is thought to be a key protein involved in the assembly of actin–membrane linkage complexes, as it is capable of interacting both with membranes and with actin filaments [1]. Membrane interaction may be mediated via binding to the cytosolic domain of transmembrane receptors of extracellular matrix proteins, e.g. integrins [2, 3], and also via direct interaction with acidic phospholipids [4–7]. The latter interaction has been demonstrated *in vitro* by a number of different techniques such as differential scanning calorimetry and Fourier-transform infrared spectroscopy [4], hydrophobic photolabelling [5], microscopy of fluorescently labelled proteins and liposomes [6] and analysis of lipid monolayers with the film balance method [7]. Talin also interacts *in vitro* with actin [5, 6, 8–12] and with vinculin [13], nucleates actin polymerization [6, 10] and induces an increase in F-actin chain stiffness [14]. An important physiological role of talin has been confirmed by *in situ* experiments showing that talin accumulates in newly formed focal contacts of fibroblasts, concomitantly with the formation of actin bundles, before detection of any other adhesion protein such as vinculin [15]. Microinjection of talin antibodies into spreading fibroblasts prevents further spreading and migration of these cells [16]. In order to assess the physiological role of direct interactions with proteins and acidic phospholipids, it is essential to determine specific binding domains in talin and to identify the amino acid residues involved.

Talin forms antiparallel rod-like homodimers [17]: electron microscopic pictures reveal a dumbbell-shaped molecule with an average length of 51 nm. This rod-like dimer configuration agrees with predictions derived from Fourier analysis of the talin sequence [18]. The dimer has been shown to be functional in nucleating actin filament formation [17]. Talin can be cleaved by calpain or thrombin into an N-terminal fragment and a C-terminal fragment with apparent molecular masses of 47 kDa and 190–200 kDa, respectively [4, 19, 20]. It has been proposed that the 200-kDa fragment contains binding sites for vinculin, integrins and actin [2, 9, 13, 21] but, except for vinculin [13], the precise locations are still lacking. Muguruma et al. [9] presented some preliminary evidence that the 200-kDa fragment binds to polymerized actin by applying a centrifugation assay. Functional effects of this fragment on actin polymerization have so far not been investigated and little is known about the binding properties and the functional role of the 47-kDa domain. According to sequence analysis of the murine protein, the 47-kDa domain shows similarities to the membrane-binding domain of protein 4.1 and ezrin [22]. Unexpectedly, in view of this, the 200-kDa, but not the 47-kDa fragment, was reported to interact with integrins [2, 21].

We have now investigated lipid and actin interactions of the two purified fragments generated by thrombin cleavage of platelet talin and report on distinct functional properties of the two domains. A preliminary report of part of this work has been published in abstract form [23].

*Correspondence to* V. Niggli, Department of Pathology, University of Bern, Murtenstr. 31, CH-3010 Bern, Switzerland

*Abbreviations.* $^{3}$H-labelled phosphatidylcholine analogue, 1-palmitoyl-2-{11-[3-(trifluoromethyl-diazirinyl)phenyl][2-$^{3}$H]undecanoyl}-*sn*-glycero-3-phosphocholine; $^{125}$I-labelled phosphatidylcholine analogue, 1-palmitoyl-2-{decanedioyl-mono-[2-[$^{125}$I]iodo-4-(3-trifluoromethyl-3*H*-diazirin-3-yl)benzyl]ester}-*sn*-glycero-3-phosphocholine; Nbd-actin, 7-chloro-4-nitro-benzeno-2-oxa-1,3-diazole–actin.

## MATERIALS AND METHODS

### Materials

The $^{125}$I-labelled phosphatidylcholine analogue, 1-palmitoyl-2-{decanedioyl-mono-[2-[$^{125}$I]iodo-4-(3-trifluoromethyl-3*H*-diazirin-3-yl)benzyl]ester}-*sn*-glycero-3-phosphocholine, was prepared as described [24] with a specific activity of $2\times10^3$ Ci/mmol. Phosphatidylcholine and phosphatidylserine were obtained from Lipid Products (South Nutfield, Surrey, England). Thrombin was obtained from Boehringer, Mannheim.

### Purification of proteins

Talin was purified from human platelets as described previously [10]. Actin was extracted from skeletal muscle acetone powder [25] followed by a gel filtration step [26]. Protein concentration was determined as described by Bradford [27] and purity was analyzed on SDS/polyacrylamide gels [28].

### Proteolytic cleavage of talin and isolation of fragments

Purified talin in buffer B (50 mM Tris/HCl pH 8.0, 3 mM EGTA, 0.1 mM dithiothreitol) was digested by thrombin (0.5 U/mg protein) at room temperature. After 40 min of digestion, benzamidine (to a final concentration of 10 mM) was added to the reaction mixture and the cleavage products were separated by chromatography on an FPLC anion-exchange column (mono Q, Pharmacia Fine Chemicals) and eluted by a linear gradient of 0–800 mM NaCl in buffer B.

### Actin polymerization

Actin polymerization was measured as described, by following an increase in fluorescence of a mixture of 95% actin plus 5% tagged with 7-chloro-4-nitrobenzeno-2-oxa-1,3-diazole–actin (Nbd-actin) [10]. Polymerization was started in the absence or presence of talin or talin fragments by adding F-actin buffer (2 mM Tris/HCl, pH 7.5 at room temperature, 0.2 mM $CaCl_2$, 2 mM $MgCl_2$, 0.5 mM ATP, 0.2 mM dithiothreitol, 100 mM KCl, final concentrations).

### Viscometry assays

The viscosity of actin solutions polymerizing in the absence or presence of talin or talin fragments was determined by falling ball viscometry as described [26]. The final actin concentration was 3 μM; actin polymerization was started by adding G-actin to talin at a molar ratio of 3:1 in F-actin buffer (see above). Low shear viscosity was determined after a 30-min incubation at room temperature. Data correspond to the mean of three determinations. The standard deviation was maximally 10%.

### Binding of talin and talin fragments to lipid vesicles

Phosphatidylserine or phosphatidylcholine (5 mg/ml) were swollen in 20 mM Hepes pH 7.4, 0.2 mM EGTA for 3 h at 42°C [29]. The vesicles were then centrifuged at 20000×*g* for 20 min at 4°C and the pellet was resuspended in the same buffer at 5 mg/ml. Intact talin, a mixture of the two talin fragments (0.15 mg/ml) or the purified 200-kDa fragment were dialyzed over night against 20 mM Tris/HCl pH 7.4, 0.1 mM EDTA, 15 mM mercaptoethanol. After centrifugation at 20000×*g* for 20 min at 4°C and protein determination [27], proteins (0.15 mg/ml) were subsequently incubated at room temperature for 15 min in the absence or presence of liposomes (0.5 mg/ml), 50–100 μl total volume, followed by centrifugation at 20000×*g*, 20 min, 4°C. Pellets were solubilized in 100 μl sample buffer containing 1% SDS, 15% (by vol.) glycerol, 0.001% bromphenolblue, 50 mM dithiothreitol and 62.5 mM Tris pH 6.8. Aliquots of the supernatants (50–70 μl) were mixed with the corresponding amount of the threefold-concentrated sample buffer. After heating the samples at 95°C for 5–10 min, they were applied to SDS/polyacrylamide gradient gels [28]. The amount of protein present in pellets and supernatants was quantified by scanning the bands on Coomassie-blue-stained gels.

### Hydrophobic photolabeling

Two types of liposomes containing the $^{125}$I-labelled phosphatidylcholine analogue were prepared: sonicated small unilamellar liposomes and large multilamellar vesicles. Both small and large liposomes (in 20 mM Hepes and 0.2 mM EGTA, pH 7.4) consisted either of phosphatidylserine or of phosphatidylcholine and of 0.001% (by mass of total lipid) of the $^{125}$I-labelled phosphatidylcholine analogue (25000–35000 cpm/1 μg total lipid). Small liposomes were prepared as described previously [5]; the large vesicles were prepared as described above.

Proteins were dialyzed against 20 mM Tris/Cl pH 7.4, 0.1 mM EDTA, 15 mM mercaptoethanol, followed by centrifugation at 20000×*g* at 4°C for 20 min prior to experimentation. Photolysis and SDS/PAGE were performed as described [5]. The Coomassie-blue-stained gels were dried and exposed for 4–8 days to Trimax XM films (3 M AG, Rüschlikon, Switzerland) at −70°C with intensifier screens.

### Quantitative evaluation of labeling

Protein-containing slices were cut out from Coomassie-blue-stained gradient gels, placed into 3-ml plastic tubes and radioactivity measured in an LKB 1272 Clinigamma counter. Background radioactivity obtained in the same lane was subtracted from that of the protein-containing slices. To correct for unequal protein loading, the amount of protein in the bands was evaluated by scanning the Coomassie-blue-stained gels and comparing with defined amounts of protein.

## RESULTS

### Effect of talin fragments on actin polymerization

Limited thrombin treatment of human platelet talin results in the generation of two fragments of 200 kDa and 47 kDa, comparable to the effect of calpain on this protein [19, 20]. We have purified both fragments by FPLC anion-exchange chromatography (Fig. 1). Due to the extended purification procedure, a substantial part of the 200-kDa fragment is further proteolyzed to a band of 180–185 kDa (Fig. 1, lane 2). This is however of minor significance, since the preparation containing this breakdown product still retains the capacity to interact with actin, as shown in Fig. 2. Preparations of intact talin and the 47-kDa fragment exhibit only minor proteolytic breakdown products (Fig. 1, lanes 1,3). Actin (total concentration 3 μM) containing 5% Nbd-actin was used to follow polymerization in the presence or absence of the purified 47-kDa or 200-kDa fragments. In

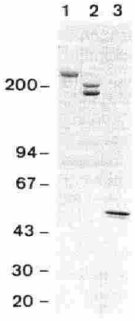


**Fig. 1. SDS/polyacrylamide gel of talin and purified talin fragments generated by thrombin treatment.** 2.5 μg purified talin (lane 1), 200-kDa fragment (lane 2) and 47-kDa fragment (lane 3) were applied to a 5–15% SDS/polyacryamide gradient gel. The numbers on the left indicate molecular masses of standard proteins in kDa.

control samples of pure actin, filament formation and filament elongation is expressed as fluorescence increase over time (Fig. 2, Ab and Bb). Nucleation, indicated by a stable fluorescence emission for approximately 50 s, is followed by filament elongation indicated by a fluorescence increase. The nucleation phase is drastically reduced when actin polymerizes in the presence of the 200-kDa fragment, and the initial rate of polymerization is markedly increased (Fig. 2, Ba). Intact talin has comparable effects on actin polymerization as measured with the same technique (inset in Fig. 2B) [10]. In contrast, the purified 47-kDa fragment does not significantly affect nucleation and the initial rate of polymerization (Fig. 2, Aa). Representative individual traces out of three or four reproducible runs are shown in Fig. 2 (A and B).

The specific interaction of the 200-kDa fragment with actin is further supported by low shear viscosity measurements of F-actin solutions under identical conditions. Actin, polymerized in the presence of 200-kDa fragment, shows a pronounced reduction in viscosity (Fig. 2C, column 4), whereas the 47-kDa fragment does not affect actin viscosity (Fig. 2C, column 2). Intact talin has the same effect on the low shear viscosity of F-actin as the 200-kDa fragment (Fig. 2C, column 3). These results were reproducibly obtained with at least two different protein preparations. The results with intact talin correspond well with previously published data demonstrating that talin induces a marked reduction in low shear viscosity when present during actin polymerization, due to the production of short filaments [6, 8].

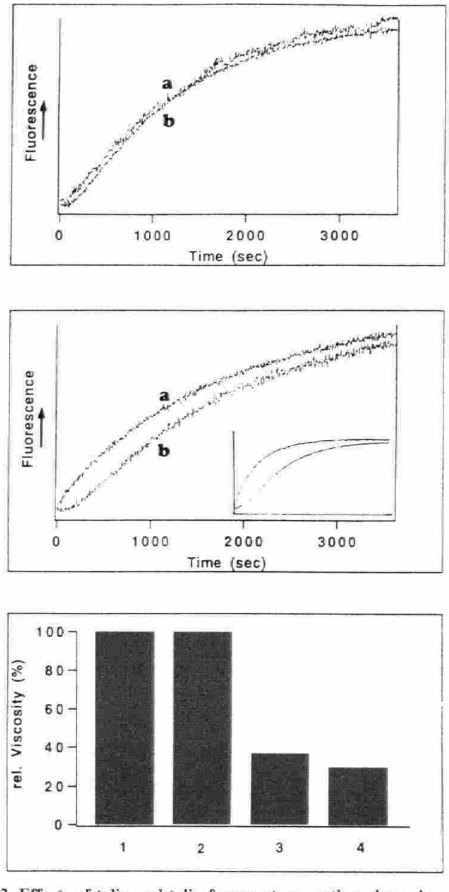


**Fig. 2. Effects of talin and talin fragments on actin polymerization.** (A, B) Fluorescence traces of 3 μM actin, with 5% Nbd-labelled actin, polymerizing in the absence of talin fragments (curves b) or in the presence of either 1 μM of 47-kDa fragment (A, curve a) or 1 μM of 200-kDa fragment (B, curve a). Inset of B: polymerization of 3 μM actin, with 5% Nbd-actin, in the absence (bottom trace) and in the presence (top trace) of 1 μM intact talin (axes as in B). Note that the 200-kDa fragment (B, curve a) induces a significant reduction in nucleation time and increases initial rate of polymerization whereas the 47-kDa fragment (A, curve a) lacks these effects. (C) The influence of intact talin (column 3), the 47-kDa fragment (column 2) or the 200-kDa fragment (column 4) in a 1:3 molar ratio on the relative viscosity of 4 μM actin. A strong reduction of the relative viscosity of pure actin (column 1) is only obtained when intact talin or the 200-kDa fragment is added; the 47-kDa fragment has no effect.

## Interaction of talin fragments with liposomes: co-sedimentation experiments

Tight interaction of talin with lipid bilayers was observed in experiments using non-equilibrium conditions, that is, gel filtration chromatography of complexes of talin with small unilamellar liposomes. These experiments were performed as described previously for vinculin and α-actinin [30]. We found that 64–80% of talin co-elutes with the peak of phosphatidylserine liposomes appearing in the void volume, under low salt conditions and (in contrast to large liposomes, see below) also in the presence of 130 mM KCl and 1 mM $MgCl_2$ (not shown). Talin thus interacts with much higher affinity with small unilamellar liposomes than vinculin and α-actinin, which dissociate from the liposomes during the run [30].

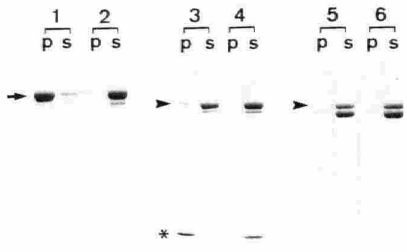


**Fig. 3. The association of intact talin and of talin fragments with large phosphatidylserine liposomes.** Talin (lanes 1,2) or a mixture of 200-kDa and 47-kDa fragments (lanes 3,4) or purified 200-kDa fragment (lanes 5,6) were incubated in the presence (lanes 1,3,5) or absence (lanes 2,4,6) of large phosphatidylserine liposomes under low salt conditions. After centrifugation, pellets (p) and supernatants (s) were analyzed on 5–15% gradient gels. Arrows indicate intact talin, arrowheads the 200-kDa fragment and asterisks the 47-kDa fragment. A significant co-sedimentation with liposomes was only observed for intact talin and the 47-kDa fragment, but not for the 200-kDa fragment.

We have also tested the ability of intact talin and of talin fragments to interact with lipids using co-sedimentation assays with large liposomes. A substantial fraction of intact talin associates tightly with acidic phospholipids, as 67–90% of total talin co-sediments with large phosphatidylserine vesicles under low salt conditions (Fig. 3, lanes 1p, 1s; see also [6]). This result was reproducibly obtained in four independent experiments. Small amounts of talin ($14 \pm 10\%$; mean ± standard deviation, $n = 4$) sediment also in the absence of lipid (Fig. 3, lanes 2p, 2s). After subtraction of the latter values from those obtained in the presence of liposomes, the amount of talin co-sedimenting with liposomes amounts to $62 \pm 11\%$ ($n = 4$) of total talin. When 130 mM KCl and 1 mM $MgCl_2$ are included in the medium, the amount of talin binding to the liposomes is reduced to $14 \pm 3\%$, $n = 3$ (after subtraction of the amount of protein sedimenting in the absence of liposomes). This amount corresponds to 24–28% of the value obtained under low salt conditions. In the same experiment, equimolar mixtures of the 200-kDa and the 47-kDa fragments were incubated with phosphatidylserine liposomes under low salt conditions (Fig. 3, lanes 3p, 3s); 65–86% of the 47-kDa fragment selectively co-sediments with the liposomes, whereas the 200-kDa fragment is recovered almost completely in the supernatant. After subtraction of the amount of protein sedimenting in the absence of liposomes, this corresponds to $65 \pm 14\%$ ($n = 4$) of the 47-kDa fragment, versus only $7 \pm 3\%$ of the 200-kDa fragment. The purified 200-kDa fragment behaves comparably to the fragment in the mixture: $12 \pm 5\%$ ($n = 3$) co-sediments with liposomes under low salt conditions (Fig. 3, lanes 5p, 5s). In comparison, 3% of a control protein, bovine serum albumin, co-sediments with phosphatidylserine vesicles under the same conditions. Note that the 200-kDa fragment in the mixture shows little degradation, whereas further proteolysis to a 185-kDa polypeptide appears to occur during purification on FPLC mono Q columns. Neither fragment binds significantly to liposomes (Fig. 3, lanes 5p, 5s). Interestingly, in the presence of 130 mM KCl and 1 mM $MgCl_2$, binding of the 47-kDa fragment to the liposomes is much less reduced than the binding of talin: $52 \pm 5\%$ ($n = 3$) of the total 47-kDa fragment co-sediments with liposomes under these conditions, corresponding to 67–100% of the values obtained under low-salt conditions in the same experiment. Liposome interaction is dependent on the presence of acidic phospholipids since no significant sedimentation of intact talin or any of the fragments was observed in the presence of phosphatidylcholine vesicles (not shown). The 47-kDa protein fragment thus has retained the lipid-binding properties of intact talin.

### Interaction of talin fragments with liposomes: hydrophobic photolabeling

Intact talin has been shown to insert partially into lipid bilayers containing acidic phospholipids by using a photoactivatable $^3$H-labelled phosphatidylcholine analogue, 1-palmitoyl-2-{11-[3-(trifluoromethyl-diazirinyl)phenyl][2-$^3$H]undecanoyl}-*sn*-glycero-3-phosphocholine, with the reactive group on its apolar portion [5]. We have now used a iodinated compound of comparable structure and properties, 1-palmitoyl-2-{decanedioyl-mono-[2-[$^{125}$I]iodo-4-(3-trifluoromethyl-3*H*-diazirin-3-yl)benzyl]ester}-*sn*-glycero-3-phosphocholine, to complement the lipid-binding studies and to extend the investigations on the talin fragments described above. As shown in Table 1, intact talin, when incubated and photolyzed under low salt conditions in the presence of small unilamellar liposomes containing phosphatidylserine and trace amounts of photolabel, incorporates significant amounts of radioactivity (0.14% of total label), comparable to the results obtained with the $^3$H-labelled analogue [5]. A control protein, bovine serum γ-globulin, under the same conditions incorporates 0.01–0.03% of total label (Table 1). Intact talin is also photolabeled when incubated in the presence of large multilamellar phosphatidylserine liposomes (Fig. 4, lanes A,a; Table 1) although to a lesser degree, very likely because much less lipid surface is available in this system, and because liposome surface curvature is reduced. When an equimolar mixture of the two fragments is incubated and photolyzed in the presence of large phosphatidylserine vesicles, the 47-kDa fragment is selectively labelled, dependent on photolysis, whereas the 200-kDa fragment does not incorporate significant amounts of label (Fig. 4, lanes B,b, C,c, D,d; Table 1). In the experiment shown in Fig. 4, intact talin incorporated 64–84 cpm/10 μg protein. The 47-kDa fragment generated from 10 μg intact talin incorporated comparable amounts of radioactivity (70 cpm) whereas the 200-kDa fragment analyzed in the same lane contained only 5 cpm. The 47-kDa polypeptide domain thus retains the lipid-binding capacity of the intact molecule. Selective labeling of the 47-kDa domain was reproducibly obtained in three independent experiments (Table 1).

In summary: both centrifugation experiments and photolabeling studies using large liposomes thus clearly demonstrate that it is the 47-kDa polypeptide domain which strongly and selectively interacts with acidic phospholipid bilayers, when compared with intact talin.

## DISCUSSION

We have presented convincing evidence that the two polypeptide domains generated by thrombin cleavage of human platelet talin retain specific functions: the larger frag-

**Table 1. Hydrophobic photolabeling of intact talin and talin fragments: quantitative evaluation.** Hydrophobic photolabeling was performed using either small or large phosphatidylserine liposomes under low salt conditions as described in Materials and Methods and in the legend of Fig. 4. IgG was used as a control protein. Indicated values correspond to the radioactivity incorporated into 10 μg purified protein. For the mixture of 47-kDa and 200-kDa fragments, radioactivity incorporated into the fragments generated from 10 μg talin was measured; n.d. = not determined.

| Liposomes | Expt | Photolysis | $^{125}$I incorporated into | |
|---|---|---|---|---|
| | | | talin | IgG |
| | | | cpm/10 μg | |
| Small | 1 | + | 1640 | n.d. |
| | 2 | + | 1560 | 90 |
| | 3 | + | 1320 | 210 |

| Liposomes | Expt | Photolysis | $^{125}$I incorporated into | | | |
|---|---|---|---|---|---|---|
| | | | talin | purified 200-kDa fragment | mixture of fragments | |
| | | | | | 47-kDa | 200-kDa |
| | | | cpm/10 μg | | | |
| Large | 4 | + | 64–84 | 5 | 70 | 5 |
| | | − | n.d. | n.d. | 11 | 5 |
| | 5 | + | 25 | 13 | 23 | 5 |
| | | − | n.d. | 0 | 4 | 0 |
| | 6 | + | 305 | n.d. | 60 | 23 |
| | | − | 0 | n.d. | 6 | 0 |

ment (200 kDa) is responsible for actin interaction and nucleation of filament formation, whereas the smaller fragment (47 kDa) interacts with membranes.

The 200-kDa domain carries a net negative charge, is rich in α-helix, exhibits a high content of hydrophobic and aromatic residues (40%) and carries a highly charged C-terminal region [18, 22]. We have presented evidence that this fragment retains the capacity to interact with actin, as was already suggested by Muguruma et al. in 1990 [9], and hence is capable of nucleating actin filament growth and reducing the viscosity of F-actin solutions by shortening the average actin filament length (Fig. 2), as does intact talin [4, 6, 8]. Talin, according to sequence analysis of the murine protein, carries no typical actin-binding domain comparable to those found in spectrin or α-actinin [22]; the amino acid residues involved in actin interaction have not yet been identified. Talin nucleates actin polymerization even in the presence of bound vinculin, suggesting that the two binding sites may not be closely adjacent [5].

For the 47-kDa subdomain, a pI of 8.43 was calculated based on the sequence of the murine protein [22] and about 33% of its amino acids have hydrophobic or aromatic side chains [22]. The 47-kDa domain does not interact with actin but has retained the lipid-binding capacity of the intact molecule, as demonstrated by its selective interaction with large liposomes and by its selective labeling by a bilayer-inserted photoactivatable lipid. Evidence presented for the physical interaction of the 47-kDa fragment with liposomes agree well

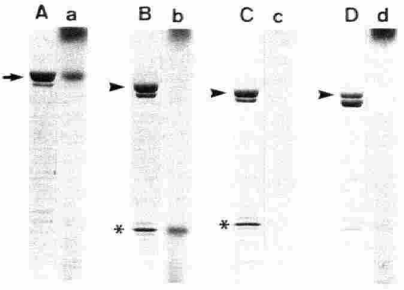


**Fig. 4. Hydrophobic photolabeling of talin and talin fragments.** Talin (lanes A,a) or a mixture of 200-kDa and 47-kDa fragment (lanes B,b, C,c) or 200-kDa fragment alone (lanes D,d) were incubated with large liposomes consisting of phosphatidylserine and trace amounts of the $^{125}$I-labelled phosphatidylcholine analogue for 15 min at room temperature under low salt conditions (0.15 mg/ml protein; 0.5 mg/ml lipid). Samples A,a, B,b and D,d were photolyzed whereas sample C,c was not photolyzed prior to application to a 5–15% gradient gel. Lanes A–D, Coomassie-blue-stained gel; lanes a–d, the corresponding autoradiogram. The arrow indicates intact talin, arrowheads the 200-kDa fragment and asterisks the 47-kDa fragment. Intact talin and the 47-kDa but not the 200-kDa fragment are labeled, dependent on photolysis.

with hydrophobic photolabeling, demonstrating that labeling is indeed indicative of a close lipid bilayer interaction of the fragment and does not occur in solution. The 200-kDa fragment is neither labeled nor does it interact with large liposomes when incubated together with the small 47-kDa fragment (Figs 3 and 4). Talin thus definitely contains at least one functional lipid-binding site in the 47-kDa domain. The 200-kDa fragment under less stringent conditions (small, highly curved unilamellar liposomes) shows some capacity to interact with lipid bilayers, as found with both hydrophobic photolabeling and gel filtration chromatography (V. Niggli and G. Isenberg, unpublished observations). This finding may be due to the high content in hydrophobic and aromatic residues. Interaction of the 47-kDa fragment appears to occur both via electrostatic and hydrophobic forces, as the interaction is dependent on the presence of acidic phospholipids and as labeling by lipid probes is indicative of partial insertion into the lipid bilayer. The basic 47-kDa domain may, in a first step, bind electrostatically to bilayers containing acidic phospholipids, followed by a secondary conformational change and insertion into the bilayer. Possibly membrane insertion of this domain occurs in a manner comparable to that of the enzyme prostaglandin $H_2$ synthase-1. Based on X-ray crystallography, an amphipathic helix of this enzyme has been suggested to insert into only one leaflet of the bilayer [31]. Interestingly, the 47-kDa fragment interacts much better with liposomes at physiological salt concentrations than the intact protein, suggesting that the 200-kDa domain has an inhibitory influence on the lipid interaction of the small 47-kDa domain under these conditions. Possibly, *in situ* mechanisms exist which could modulate this inhibition, such as reversible phosphorylation. Talin has been reported to be a substrate of various kinases [1].

Amino acid residues 165–373 of the 47-kDa talin fragment exhibit 20% identity with the N-terminal domain of protein 4.1 which has been proposed to mediate membrane

interaction of this protein [22]. Indeed, the 30-kDa fragment of protein 4.1 which carries these similar sequences has been shown to interact selectively with phosphatidylserine liposomes [32], a finding which could be correlated with our results concerning the function of the N-terminal domain of talin. The identification of two functionally distinct domains in talin involved in (a) lipid and (b) actin interaction agrees well with the notion that talin can nucleate actin filament growth at the bilayer surface [6].

This may be of physiological relevance since talin appears to play an important role in initiating actin filament growth in motile cell protrusions [15]. Direct bilayer interactions could serve, on the one hand, to concentrate the protein at the membrane in the correct orientation and, on the other hand, to facilitate and modulate interactions with transmembrane receptors such as integrins [33]. It has been shown by microinjection of fluorescently labeled talin fragments into fibroblasts that both the 200-kDa and the 47-kDa subdomains contain binding sites that direct these fragments to focal contacts [34]. For the 200-kDa fragment, the relevant binding sites may be provided by vinculin and integrins. However, it is not yet known how the 47-kDa fragment is targetted to focal contacts, since no specific protein-binding sites have yet been identified. The lipid-binding site obviously would not suffice to mediate accumulation in a specific membrane site.

Other cytoskeletal proteins, e.g. ezrin, also exhibit a domain similar to the N-terminal domains of talin and protein 4.1 [22]. The N-terminal domain of ezrin, when transfected into kidney cells, has been shown to locate specifically to the dorsal plasma membrane, but lacks the capacity to interact with the cytoskeleton which is retained by the C-terminal fragment [35]. For ezrin, neither a lipid-binding capacity nor partners for protein interaction near the plasma membrane are yet known.

In summary: our results represent the first evidence for a functional difference of the two major polypeptide domains of the cytoskeletal protein talin. These two functions enable the intact protein to interact simultaneously via its 47-kDa polypeptide domain with lipid bilayers and via its 200-kDa domain with actin. It will be important to investigate the correlation between functional domains and ultrastructure. It will also be necessary to identify the amino acid residues involved in bilayer interaction of the 47-kDa domain. Such studies offer the potential to directly examine the contribution of the lipid-binding domain to talin function in genetic systems.

We thank K. Mujynya-Ludunge for excellent technical assistance, Dr J. Brunner for helpful comments concerning hydrophobic photolabeling, Dr E. Sigel for helpful comments regarding the liposome studies and for critical reading of the manuscript and Prof. H. U. Keller, in whose Department the liposome experiments were performed, for continuous support. This work was supported by the Swiss National Foundation for Scientific Research (to V. N. and to Dr J. Brunner, ETH, Zurich), by the Sandoz Foundation (Basel, Switzerland) (to V. N.), by grants from *Deutsche Forschungsgemeinschaft* (SFB 266, C-5 and Is 25/7−1, to G. I.) and by NATO grant CRG 940666 (to W. H. G).

## REFERENCES

1. Isenberg, G. & Goldmann, W. H. (1992) Actin−membrane coupling: a role for talin, *J. Muscle Res. Cell Motil. 13*, 587−589.
2. Horwitz, A., Duggan, K., Buck, C., Beckerle, M. C. & Burridge, K. (1986) Interaction of plasma membrane fibronectin receptor with talin − a transmembrane linkage, *Nature 320*, 531−533.
3. Geiger, B., Salomon, D., Takeichi, M. & Hynes, R. (1992) A chimeric N-cadherin/$\beta_1$-integrin receptor which localizes to both cell-cell & cell-matrix adhesions, *J. Cell Sci. 103*, 943−951.
4. Heise, H., Bayerl, T., Isenberg, G. & Sackmann, E. (1991) Human platelet P-235, a talin-like actin binding protein, binds selectively to mixed lipid bilayers, *Biochim. Biophys. Acta 1061*, 121−131.
5. Goldmann, W. H., Niggli, V., Kaufmann, S. & Isenberg, G. (1992) Probing actin and liposome interaction of talin and talin-vinculin complexes: A kinetic, thermodynamic and lipid labeling study, *Biochemistry 31*, 7665−7671.
6. Kaufmann, S., Käs, J., Goldmann, W. H., Sackmann, E. & Isenberg, G. (1992) Talin anchors and nucleates actin filaments at lipid membranes: A direct demonstration, *FEBS Lett. 314*, 203−205.
7. Dietrich, C., Goldmann, W. H., Sackmann, E. & Isenberg, G. (1993) Interaction of NBD-talin with lipid monolayers: A film balance study, *FEBS Lett. 324*, 37−40.
8. Collier, N. C. & Wang, K. (1982) Human platelet P235: A high-*M*, protein which restricts the length of actin filaments, *FEBS Lett. 143*, 205−210.
9. Muguruma, M., Matsumara, S. & Fukazawa, T. (1990) Direct interactions between talin and actin, *Biochem. Biophys. Res. Commun. 171*, 1217−1223.
10. Kaufmann, S., Piekenbrock, T., Goldmann, W. H., Bärmann, M. & Isenberg, G. (1991) Talin binds to actin and promotes filament nucleation, *FEBS Lett. 284*, 187−191.
11. Muguruma, M., Matsumura, S. & Fukazawa, T. (1992) Augmentation of $\alpha$-actinin-induced gelation of actin by talin, *J. Biol. Chem. 267*, 5621−5624.
12. Schmidt, J. M., Robson, R. M., Zhang, J. & Stromer, M. H. (1993) The marked pH dependence of the talin−actin interaction, *Biochem. Biophys. Res. Commun. 197*, 660−666.
13. Gilmore, A. P., Jackson, P., Waites, G. T. & Critchley, D. R. (1992) Further characterization of the talin-binding site in the cytoskeletal protein vinculin, *J. Cell Sci. 103*, 719−731.
14. Ruddies, R., Goldmann, W. H., Isenberg, G. & Sackmann, E. (1993) The viscoelasticity of entangled actin networks: The influence of defects and modulation by talin and vinculin, *Eur. Biophys. J. 22*, 309−321.
15. DePasquale, J. A. & Izzard, C. S. (1991) Accumulation of talin in nodes at the edge of lamellipodium and separate incorporation into adhesion plaques at focal contacts in fibroblasts, *J. Cell Biol. 113*, 1351−1359.
16. Nuckolls, G. H., Romer, L. H. & Burridge, K. (1992) Microinjection of antibodies against talin inhibits the spreading and migration of fibroblasts, *J. Cell Sci. 102*, 753−762.
17. Goldmann, W. H., Bremer A., Häner, M., Aebi, U. & Isenberg, G. (1994) Native talin is a dumbbell-shaped homodimer when it interacts with actin, *J. Struct. Biol. 112*, 3−10.
18. McLachlan, A. D., Stewart, M., Hynes, R. O. & Rees, J. D. G. (1994) Analysis of repeated motifs in the talin rod, *J. Mol. Biol. 235*, 1278−1290.
19. Fox, J. E. B., Goll, D. E., Reynolds, C. C. & Philips, D. R. (1985) Identification of two proteins (actin-binding protein and P235) that are hydrolyzed by endogenous $Ca^{2+}$-dependent protease during platelet aggregation, *J. Biol. Chem. 260*, 1060−1066.
20. Beckerle, M. C., Burridge, K., DeMartino, G. N. & Croall, D. E. (1987) Colocalization of calcium-dependent protease II and one of its substrates at sites of cell adhesion, *Cell 51*, 569−577.
21. Simon, K. O. & Burridge, K. (1991) Characterization of the interaction between talin and the cytoplasmic domain of $\beta_1$ integrin, *J. Cell Biol. 115*, 351a (abstract).
22. Rees, D. J. G., Ades, S. E., Singer, S. J. & Hynes, R. O. (1990) Sequence and domain structure of talin, *Nature 347*, 685−689.

23. Niggli, V., Kaufmann, S., Goldmann, W. H. & Isenberg, G. (1994) Functional domains in the cytoskeletal protein talin, *Experientia 50*, A56 (abstract).
24. Weber, T., Paesold, G., Galli, C., Mischler, R., Semenza, G. & Brunner, J. (1994) Evidence for H$^+$-induced insertion of the influenza hemagglutinin HA2 N-terminal segment into the viral membrane, *J. Biol. Chem. 269*, 18353–18358.
25. Spudich, J. A. & Watt, S. (1971) The regulation of rabbit skeletal muscle contraction, *J. Biol. Chem. 246*, 4866–4871.
26. MacLean-Fletcher, S. D. & Pollard, T. D. (1980) Viscosimetric analysis of the gelation of acanthamoeba extracts and purification of two gelation factors, *J. Cell Biol. 85*, 414–428.
27. Bradford, M. M. (1976) A rapid and sensitive method for the quantitation of microgram quantities of protein utilizing the principle of protein-dye binding, *Anal. Biochem. 72*, 248–254.
28. Laemmli, U. K. (1970) Cleavage of structural proteins during the assembly of the head of bacteriophage T4, *Nature 227*, 680–685.
29. Evans, E. & Kwok, R. (1982) Mechanical calorimetry of large dimyristoylphosphatidylcholine vesicles in the phase transition region, *Biochemistry 21*, 4874–4879.
30. Niggli, V. & Gimona, M. (1993) Evidence for a ternary interaction between $\alpha$-actinin, (meta)vinculin and acidic phospholipid bilayers, *Eur. J. Biochem. 213*, 1009–1015.
31. Picot, D., Loll, P. J. & Garavito, R. M. (1994) The X-ray crystal structure of the membrane protein prostaglandin $H_2$ synthase-1, *Nature 367*, 243–249.
32. Cohen, A. M., Liu, S. C., Lawler, J., Derick, L. & Palek, J. (1988) Identification of the protein 4.1 binding site to phosphatidylserine vesicles, *Biochemistry 27*, 614–619.
33. Niggli, V. & Burger, M. M. (1987) Interaction of the cytoskeleton with the plasma membrane, *J. Membrane Biol. 100*, 97–121.
34. Nuckolls, G. H., Turner, C. E. & Burridge, K. (1990) Functional studies of the domains of talin, *J. Cell Biol. 110*, 1635–1644.
35. Algrain, M., Turunen, O., Vaheri, A., Louvard, D. & Arpin, M. (1993) Ezrin contains cytoskeleton and membrane binding domains accounting for its proposed role as a membrane-cytoskeletal linker, *J. Cell Biol. 120*, 129–139.